

WKB Across Caustics: The Screened-WKB Method

Oscar P. Bruno*

Martin D. Maas*

Abstract

We present a new methodology, based on the WKB approximation and Fast Fourier Transforms, for the evaluation of wave propagation through inhomogeneous media. This method can accurately resolve fields containing caustics, while still enjoying the computational advantages of the WKB approximation, namely, the ability to resolve arbitrarily high-frequency problems in computing times which are orders-of-magnitude shorter than those required by other algorithms presently available. For example, the proposed approach can simulate with high accuracy (with errors such as e.g. 0.1%–0.001%) the propagation of 5 cm radar signals across two-dimensional configurations resembling atmospheric ducting conditions, spanning hundreds of kilometers and millions of wavelengths in electrical size, in computing times of a few minutes in an ordinary CPU workstation.

1 Introduction

Computations of high-frequency wave propagation through inhomogeneous media play a pivotal role in diverse fields such as telecommunications, remote sensing, seismics, quantum mechanics, and optics. A wide range of methodologies have been developed over the last century for the treatment of high-frequency volumetric-propagation problems. Given that direct numerical simulation of the configurations of interest, which comprise thousands to millions of wavelengths in acoustic/electrical size, is unfeasible in 2D and even more in 3D, the proposed approaches usually contain a combination of analytic and numerical approximations.

The celebrated WKB approximation, also known as the Wentzel-Kramers-Brillouin approximation [3, 10], was the first method to obtain accurate solutions to problems involving propagation over large distances, and is based on the introduction of a system of ray-coordinates, over which the amplitude and phase of the solution exhibit slow variations. However, the WKB approximation can break down in certain situations, particularly when the ray mapping becomes singular (i.e. at caustics). Many approaches have been proposed over time to overcome this limitation, most notably the KMAH-index theory, according to which a correction can be incorporated after the caustic, of the form $(-i)^m$, where the constant m depends on the number and type of caustics that the ray has traversed. This formulation still breaks down at caustics, is inaccurate near caustics, and, given its complexity, it is seldom used in practice.

Another notable approach to solve these type of problems is provided by the parabolic approximation introduced in [11], together with its many subsequent versions and improvements, including the wide-angle approximation [7]. The method of phase-screens [16], in turn, which assumes a constant refractivity profile along each vertical volumetric screen, is applicable for certain restricted sets of configurations. While, unlike the classical WKB approach, these methods are valid at and around caustics, their limitations arise from its computational cost. For example, mesh-sizes of

*Computing and Mathematical Sciences, Caltech, Pasadena, CA 91125, USA

the order of $\Delta z \approx \frac{\lambda}{4}$ and $\Delta x \approx 12.5\lambda$ are reported for propagation distances in the order of a few hundreds of wavelengths (see [9] and references therein). (Here z and x denote the vertical and range variables, respectively.) The parabolic equation methods are most often based on use of finite-difference approximations, which gives rise to associated dispersion errors, while Fourier expansions in the vertical axis are only applicable in the lowest-order parabolic approximations. The combined effect of large propagation distances, and the presence of dispersion error, and the requirement of fine spatial discretizations, can lead to extremely large computational cost, under reasonable error tolerances, for challenging configurations commonly arising in applications.

Other notable approaches include the Gaussian beams formulation, with contributions spanning from the 60's, including [2,5,8,15] among many others. This formulation is based on an additional approximation to WKB, which seeks to obtain the phase in the form of a quadratic polynomial, whose Hessian matrix is evolved along the ray. This approach eliminates ray-bunching at caustics, and produces fields which remain bounded. However, theoretical convergence as $k \rightarrow \infty$ has not been established and is believed to be slow. Moreover, the initial beam representation is a challenging optimization problem, which leads to errors of a few percent even for propagations distances of the order of a small number of wavelengths [15].

An additional approach, known as Dynamic Surface Extension (DSE, see [13,14]), can successfully propagate wavefronts in a Cartesian discretization. However, the amplitude computations present the same limitations as the classical WKB approximation. Finally, the Kinetic Formulation [6] views each ray tracing equation as describing the motion of a "particle" (e.g. photon, phonon). This method presents severe computational difficulties, as the initial conditions and solutions are given in terms of Wigner measures, a δ -function that vanishes for incorrect directions p . The approach put forth in this paper, on the other hand, is based on the WKB approximation, and overcomes the limitations posed by caustics by resorting to a family of curves (or screens) on which the total field is decomposed in Fourier modes. Each mode is then propagated for large electrical distances (i.e. $20,000\lambda$ in the example considered in Figure 5) which are also short enough that the presence of caustics is avoided for each Fourier mode.

2 The Screened-WKB Method

We consider, as a model problem, the scalar Helmholtz equation

$$\Delta u(\mathbf{r}) + k^2 \varepsilon(\mathbf{r})u(\mathbf{r}) = 0 \quad (1)$$

$$u = u^s + u^{\text{inc}} \quad (2)$$

$$\lim_{r \rightarrow \infty} r \left(\frac{\partial u^s}{\partial r} - iku^s \right) = 0, \quad (3)$$

whose character at high frequencies presents challenges often found in diverse fields, such high-frequency electromagnetism, acoustics, seismics and quantum mechanics.

The proposed screened-WKB approach first introduces a family of curves (or screens) Γ_q , for $q = 0, 1, \dots, N_s$, as depicted in Figure 1. The method proceeds by propagating the solution from one screen to the next on the basis of Fourier expansions on the screens Γ_q and applications of the classical WKB approach for each separate Fourier mode.

For conciseness, we consider planar screens of the form $\Gamma_q = \{(x_q, z) : z \in (z_a, z_b)\}$. The initial conditions on Γ_0 are user-prescribed, and given by:

$$u|_{\Gamma_0} = u^{\text{inc}}|_{\Gamma_0} \quad (4)$$

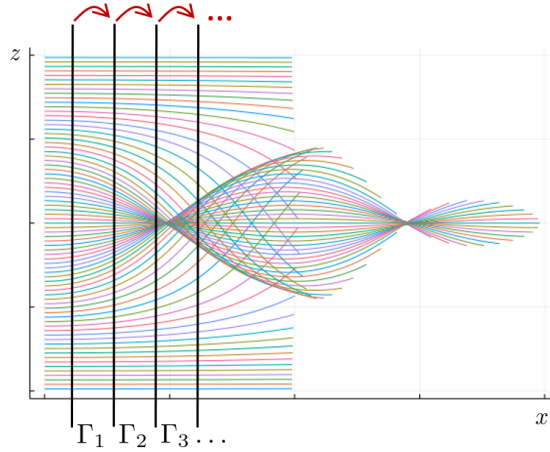


Figure 1: Schematics underlying the proposed S-WKB method. Here and throughout this paper flat screens Γ_q are used, but curved screens could alternatively be utilized, if convenient.

As we seek to employ the classical WKB approximation between Γ_q and Γ_{q+1} for each q , we seek to represent the incident field on each screen Γ_q , arising from propagation of the field from Γ_{q-1} (or given by (4) for $q = 0$) by expressions of the form

$$u(x, z) \approx \sum_{n=-N/2}^{N/2-1} A_n^q(x, z) \exp(ik\psi_n^q(x, z)). \quad (5)$$

In other words, this expression corresponds with sums of WKB-expansions.

2.1 The z -periodic case

We will first introduce the proposed approach under the assumption that the incident field and the solution are z -periodic functions, which will enable the construction of a simple algorithm and provide some numerical results. Under such hypothesis, the method can begin with a “vertical” DFT, and provide a Fourier representation that is exploited to . In subsequent sections, a generalization based around the Fourier Continuation strategy will be presented, that is not only more general but also computationally more efficient, along with specific methods to deal with homogeneous Dirichlet and Neumann boundary conditions.

2.1.1 From FFTs to WKB expansions

Assuming the incident field and the solution are periodic in z (In particular, this also includes cases wherein the solution decays rapidly outside a bounded interval in the z variable.), for a given screen Γ_q , a “vertical” DFT can be used by introducing an equi-spaced grid

$$\{z_m : m = -N/2, \dots, N/2 - 1\} \quad (6)$$

in the interval $[z_a, z_b]$. Performing an FFT yields

$$w_j^q = \sum_{m=-N/2}^{N/2-1} u(x_q, z_m) e^{-ijz_m}. \quad (7)$$

Then, we can re-express the field $u(x_q, z)$ in terms of an inverse DFT:

$$u|_{\Gamma_q} \approx \frac{1}{N} \sum_{m=-N/2}^{N/2-1} w_j^q e^{ijz_m}, \quad (8)$$

Now, by introducing the functions $\psi_n^q(x_q, z)$ defined by

$$\psi_n^q(x_q, z) = \left(z + \frac{z_b - z_a}{2} \right) \frac{2n\pi}{k(z_b - z_a)}. \quad (9)$$

we obtain an expression of the form

$$u|_{\Gamma_q} \approx \frac{1}{N} \sum_{m=-N/2}^{N/2-1} w_j^q e^{ij\psi_n^q(x_q, z_m)}, \quad (10)$$

which in turn, corresponds to an expression of the form (5) evaluated in a discretization of the points of the screen Γ_q .

So far the proposed method is physically-exact. Under the assumptions that the incident field propagates mostly in the x direction, the resulting fields should be slowly-varying in the z direction, which makes the FFT approach viable. However, the problem of propagating each term in the expansion (10) up to the next screen Γ_{q+1} , involves highly oscillatory functions. In order to do this, we seek asymptotic solutions to equation (1). In a procedure which is equivalent to the WKB expansion (see e.g. [9, chapter 3]), we consider trial solutions of the form

$$u(r) = A(r) \exp[ik\psi(r)] \quad (11)$$

and expand the amplitude in inverse powers of the wavenumber,

$$A(r) = A_1(r) + \frac{A_2}{ik} + \frac{A_3}{(ik)^2} + \dots \quad (12)$$

Replacing the trial solution (11) in the Helmholtz (1) results in

$$\Delta u(r) + k^2 \varepsilon(r) u(r) = k^2 [\varepsilon(r) - \psi(r)] \quad (13)$$

$$+ ik [2\nabla\psi \cdot \nabla A_1 + A_1 \Delta\psi] \quad (14)$$

$$+ \Delta A \quad (15)$$

Up to degree 2 in k , we obtain the Eikonal equation and the transport equations:

$$(\nabla\psi)^2 = \varepsilon(r) \quad (16)$$

$$2\nabla\psi \cdot \nabla A + A\Delta\psi = 0 \quad (17)$$

2.1.2 From the Γ_q screen to Γ_{q+1} via WKB

The algorithm proceeds by propagating each mode in the expansion (10) by means of WKB expansions. In other words, in order to perform this asymptotic procedure up to order $O(\frac{1}{k^2})$, we must solve the eikonal and transport equations (16) and (17) for each mode. Interestingly, the proposed approach is compatible with any solution strategy for this problem.

For completeness, in the present section we discuss a high-order solver based on characteristics tracing with ODE solvers and piecewise interpolation.

As a first step, the system of characteristics equations for the system (16) and (17) (obtained in Appendix A) is solved by employing numerical ODE solvers.

In order to obtain initial conditions for the eikonal equation (16) for each mode of (10) on Γ_q , we resort to (9), while the initial conditions for the transport equation (17) are given by the Fourier amplitudes w^q . We then have the following set of initial conditions

$$\partial_z \psi_n(x_q, z) = \frac{2n\pi}{k(z_b - z_a)} \quad (18)$$

$$\partial_x \psi_n(x_q, z) = \sqrt{\varepsilon(x_q, z) - \left(\frac{2n\pi}{k(z_b - z_a)} \right)^2} \quad (19)$$

$$A(x_q, z) = w^q \quad (20)$$

Applying an ODE solver to the system of characteristics (equations (35) and (38) in the Appendix A), yields a finite number of adequately spaced geometrical-optics rays, and corresponding values of ψ_n and A_n along the rays for the n -th mode.

Standard interpolation procedures can then be used on Γ_{q+1} to obtain approximate values of u on the 1D Cartesian grid (x_{q+1}, z_m) ($-\frac{N}{2} \leq n \leq \frac{N}{2} - 1$) on Γ_{q+1} :

$$u(x_{q+1}, z_m) \approx \sum_{n=-N/2}^{N/2-1} A_n^q(x_{q+1}, z_m) \exp(ik\psi_n^q(z_m)). \quad (21)$$

The next iteration of the algorithm can then be initiated by expanding $u(x_{q+1}, z)$ in a Fourier series along Γ_{q+1} . Repeating this procedure for all screens, the field u over the domain of interest can be obtained. When desired, additional interpolation points can be added for visualization purposes.

Remark. *Importantly, by adequately selecting the spacing of the screens Γ_q , it can be ensured that all the modes $-\frac{N}{2} \leq n \leq \frac{N}{2} - 1$ propagate to the next screen Γ_{q+1} without incurring caustics.*

2.1.3 Summary of the algorithm for the z -periodic case

The overall algorithm can thus be summarized as follows:

Algorithm 1 Screened WKB

Expand u_{inc} with a vertical FFT (7), to obtain (5).

Solve Eikonal and transport equations for each ψ_n, A_n .

Interpolate ψ_n, A_n to a Cartesian grid.

Perform sum over n to obtain new incident field on next screen.

Remark. *The method described for the periodic case, is not only limited to such configurations, but it also has a computational cost of $O(n^2)$, where n is the number of points required for the discretization of the z variable. This factor can be the source of an important limitation for problems that are large enough in the vertical dimension.*

2.2 Overlapping Fourier-Continuation SWKB

We now present a generalized method, based on an overlapping Fourier Continuation decomposition, that produces representations of similar form to (5), which is applicable to periodic and non-periodic

functions. As a first step, in this section we consider the case in which the incident field u_{inc} and resulting solution between two consecutive screens vanishes in a neighborhood of the domain boundary; the subsequent treatment of boundary conditions is discussed in Section .

We thus consider an overlapping-grid decomposition of the interval $[z_a, z_b]$, that is, a collection of “overlapping patches” of the form $[a_p, b_p] \subset [z_a, z_b]$ with $a_{p+1} < b_p$, together with a uniform grid $\{z_m^p : 0 \leq m \leq M\}$ defined on each of those patches. The method proceeds by obtaining a Fourier decomposition on each patch by means of the Fourier Continuation method [1, 4], which produces accurate Fourier expansions of non-periodic smooth functions—which play a similar role to that of (8) in the periodic context. As the FC method is applied in each patch, we obtain, in the overlapping regions, two simultaneous representations of the same function. In order to obtain a single representation which remains smooth throughout $[z_a, z_b]$, we employ a smooth partition of unity which vanishes at the endpoints of each patch. This process results in a representation that closely resembles (10):

$$u|_{\Gamma_q} \approx \sum_{p=0}^P S^p(z) \sum_{m=-N/2}^{N/2-1} \frac{w_j^{q,p}}{N} e^{ij\psi_n^{q,p}(x_q, z_m)}, \quad (22)$$

In particular, we can now apply the classical WKB expansion to each Fourier mode at each patch, as previously done in the periodic case, by considering initial conditions $\frac{S^p(z)}{N} w_j^{q,p}$ for the the amplitud terms in the transport equation A .

2.3 Treatment of non-periodic boundary conditions

The continuation methodology put forth in previous sections enables the treatment of non-periodic boundary conditions. In this section, we present methods to deal with either homogeneous Dirichlet or Neumann conditions. The proposed approach is based on constructing a solution in an extended domain and later reflecting it in such a way that the boundary condition is satisfied. As a first step, we consider a “reflected” permittivity $\tilde{\epsilon}(r)$ along the boundary, given by

$$\tilde{\epsilon}(x, z) = \begin{cases} \epsilon(x, z) & z \in [z_a, z_b] \\ \epsilon(x, 2z_b - z) & z > z_b \\ \epsilon(x, 2z_a - z) & z < z_a \end{cases} \quad (23)$$

After a solution u_{tot} is produced in the extended domain, we can obtain a solution for the Dirichlet (resp. Neumann) problem by defining

$$u_{\text{reff}}(x, z) = u_{\text{tot}}(x, z) \pm u_{\text{tot}}(\tilde{x}, z) \quad (24)$$

where $\tilde{x} = 2z_a - z$ in a neighborhood of the endpoint z_a , or $\tilde{x} = 2z_b - z$ in a neighborhood of z_b . It is easily verified that u_{reff} satisfies Neumann (resp. Dirichlet) boundary conditions. However, this reflection procedure also introduces a singular derivative at each of the endpoints, which, in view of the Gibbs phenomenon, could lead to large errors in our Fourier representations. This means that this reflection procedure cannot be employed in patches that contain the boundaries. This is not a limitation, as the reflection can be applied to all other patches, leaving the boundary patches unmodified until all iterations are completed, to produce the final reflection at the end of the algorithm.

3 Numerical results

In order to evaluate the accuracy of the proposed S-WKB method, we compare with solutions obtainable by means of separation of variables (see Section 3.1) for x -invariant permittivity. Im-

portantly, the method described in Section 3.1 is physically-exact—i.e., which contain no approximations to (1) other than those inherent in the well established numerical solver utilized. For a number of test cases we use the exponential permittivity model

$$\varepsilon(z) = 1 + ae^{-bz^2} \quad (25)$$

Together with an incident field given by a Gaussian beam

$$u_{\text{inc}}(x, z) = \int_{-\infty}^{\infty} e^{i\sqrt{k^2 - \beta^2}x + i\beta z} e^{-\frac{\beta^2}{\sigma^2}} d\beta \quad (26)$$

wherein the integral in the variable β is evaluated via standard numerical integration techniques.

3.1 High-order reference solutions for x -invariant permittivity

In order to assess the accuracy of the proposed approach, reference solutions obtained for x -invariant permittivity (i.e. permittivity of the form $\varepsilon(x, z) = \varepsilon(z)$) are used, for which exact solutions to (1) may be obtained via separation of variables:

$$u(x, z) = \sum_{i=0}^{\infty} a_i e^{i\alpha_i x} \phi_i(z). \quad (27)$$

Substituting (27) in (1) leads to

$$\sum_{i=0}^{\infty} (-\alpha_i^2 + \phi_i''(z) + k^2\varepsilon(z)) a_i e^{i\alpha_i x} = 0. \quad (28)$$

Using the orthogonality of the complex exponential functions we then obtain

$$(-\alpha_i^2 + \phi_i''(z) + k^2\varepsilon(z)) a_i = 0. \quad (29)$$

It follows that the non-zero coefficients α_i in (27) satisfy the Sturm-Liouville problem:

$$\phi_i''(z) + k^2\varepsilon(z)\phi_i(z) = \alpha_i^2\phi_i(z) \quad (30)$$

for given boundary conditions on z , which depend on the configuration being considered. The resulting Sturm-Liouville problem can be discretized with high-order spectral methods. For illustration purposes, in the present paper we employed the spectral eigensolver [12], which is available in the ApproxFun.jl Julia package. In the context of the examples considered in the present paper either periodic or homogeneous Dirichlet and Neumann boundary conditions need to be enforced.

A separation-of-variables solution method may be obtained that matches the series expansion (27) to given initial conditions at $x = 0$:

$$u_{\text{inc}}(z) = \sum_{i=0}^{\infty} a_i \phi_i(z). \quad (31)$$

Given that the eigenfunctions $\{\phi_i\}$ are orthogonal in $[z_a, z_b]$ we obtain

$$a_i = \frac{\int_{z_a}^{z_b} u_{\text{inc}}(z) \phi_i(z) dz}{\int_{z_a}^{z_b} \phi_i(z)^2 dz}. \quad (32)$$

These integrals can be calculated numerically using suitable quadrature rules, which in particular are handled adaptively by the ApproxFun.jl package. Given the coefficients a_i , the solution in the entire domain can be evaluated using (27).

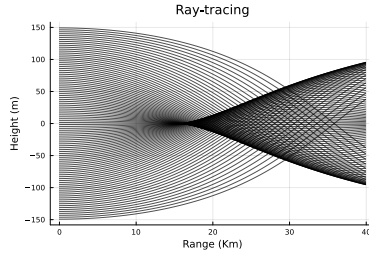


Figure 2: Example 1: Ray-tracing leading to a single cusp caustic.

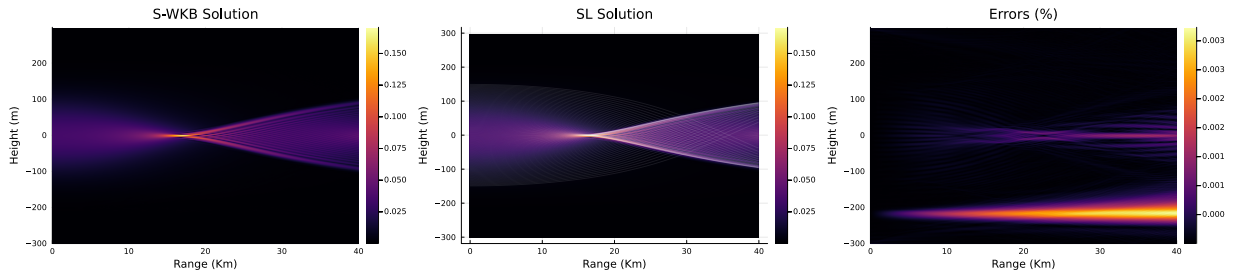


Figure 3: S-WKB solution (left), and physically-exact separation-of-variables solution with superimposed geometrical-optics rays (center), with $k = 125$, along a propagation domain 40 km (800,000 wavelengths) in range, and errors (right) for the “single-caustic” solution a relative error of the order of 10^{-5} was obtained throughout the propagation domain

3.2 Results for the z -periodic case

In our first example we consider the permittivity model (25) with parameters $a = 10^{-4}$ and $b = 10^{-4}$ —which, at C-band, results in a configuration that gives rise to a single caustic of cusp type for the first 40km (800,000 wavelengths) in horizontal propagation range. The geometrical optics rays for this configuration are displayed in Fig. 2. It can be seen that the configuration presents a number of caustics: a single point of focusing, together with an envelope of rays. The S-WKB solution, alongside the Sturm-Liouville solution with superimposed ray-tracing, and the corresponding relative errors, are depicted in Fig. As shown, the relative errors for this configuration are of the order of 10^{-5} . Employing 400 Fourier modes and a total of 40 screens, the S-WKB solution in this case was obtained in a computing time of 2 minutes in a single-core.

For our next example we consider a “ducting” configuration, in which the incident Gaussian beam is tilted by an angle of 0.2° , and where the Gaussian permittivity (25) was used with parameters $a = 10^{-4}$ and $b = 10^{-3}$ —in such a way that the energy is contained within a bounded interval along the z axis. The geometrical-optics rays form a complex system with multiple caustics, as depicted in Fig. 4. We consider the propagation of this signal over a range of 200km (4 million wavelengths) in range, which was obtained with an error of 0.1% in a 4 minute single-core computation.

3.3 Results for non-periodic cases

The numerical results based on FC representations are similar in nature to that of the periodic case, with two notable exceptions: non-periodic boundary conditions may be considered, including boundary reflections, on one hand; and problems with substantially larger heights can be tackled, in view of the reduced computational complexity of the method. The corresponding numerical

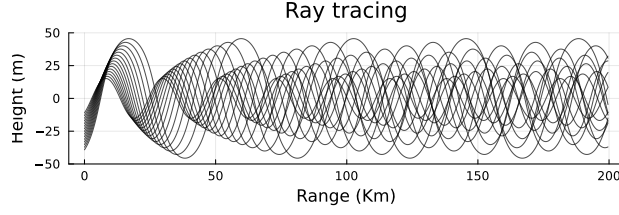


Figure 4: Geometrical optics rays for a “ducting” configuration.

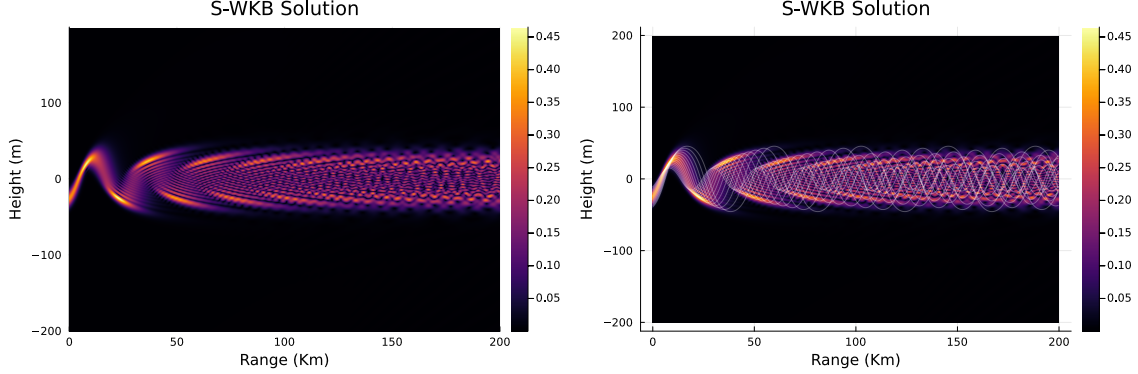


Figure 5: “Multiple caustics” test case depicting an idealized “ducting” configuration. S-WKB field values (top), and field values with super-imposed geometrical-optics rays (bottom). The geometrical optics rays are depicted in Figure 4.

results are displayed in Figures 6 and 7

In Fig. 7 we consider a simplified version of a super-refractive atmosphere with permittivity given by

$$\varepsilon(z) = 1.0004 - ae^{-bz^2} \quad (33)$$

with $a = 1.5 \times 10^{-4}$, $b = 1.5 \times 10^{-4}$.

A The system of characteristics for the eikonal and transport equations

Given that (16)-(17) is a system of first-order equations, it can be solved with the method of characteristics. Following [Garabedian], after introducing the ray coordinates $x(s, t), z(s, t)$, the following system of ordinary differential equations is obtained

$$\psi_x^2 + \psi_z^2 - \varepsilon(x, z) = 0 \quad (34)$$

results in

$$\begin{cases} \partial_t x = 2\psi_x \\ \partial_t z = 2\psi_z \\ \partial_t \psi = 2\varepsilon \\ \partial_t \psi_x = \varepsilon_x \\ \partial_t \psi_z = \varepsilon_z \end{cases} \quad (35)$$

where all quantities are evaluated along the characteristics.

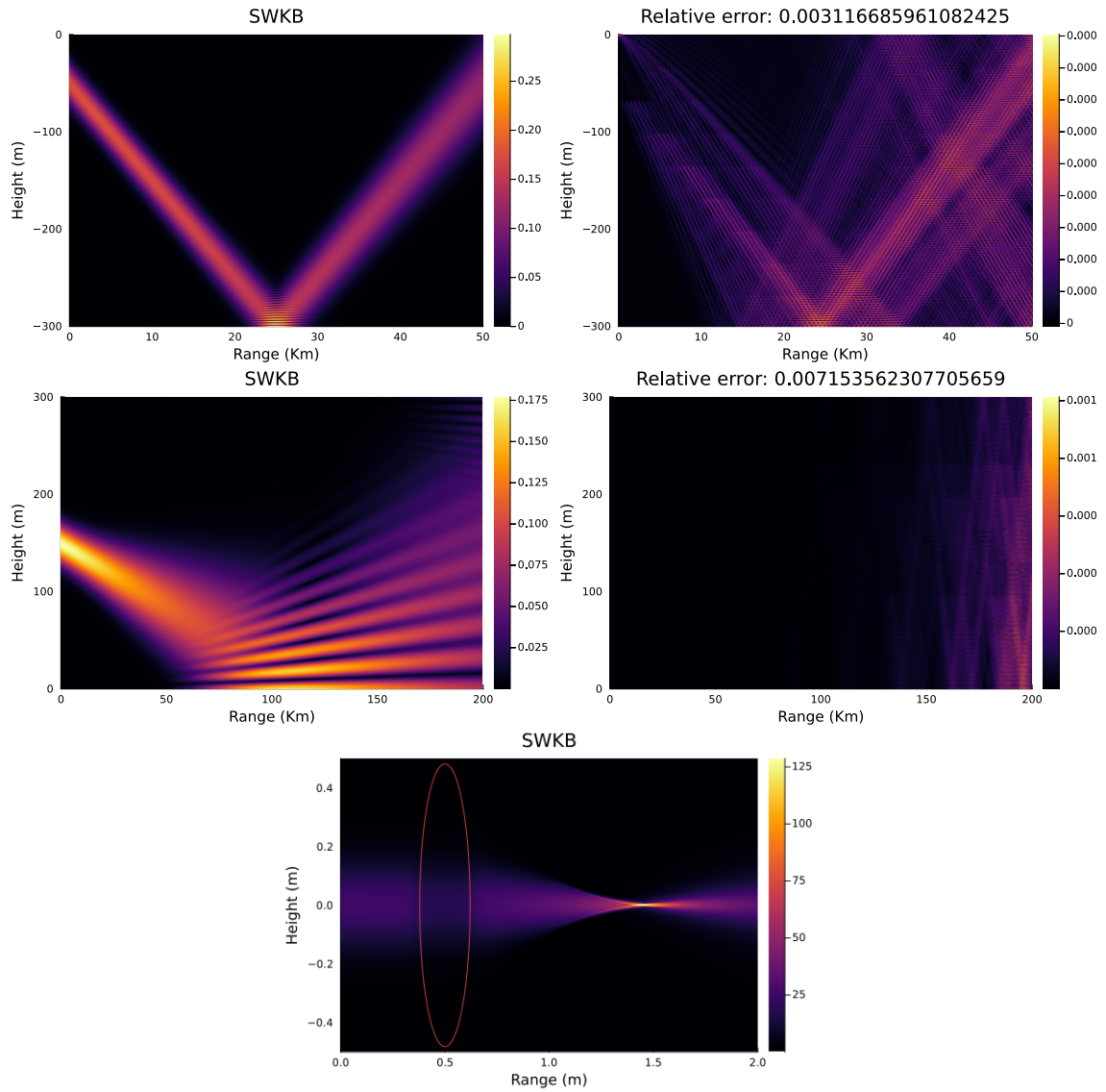


Figure 6: Beam reflection for a high incidence angle, beam splitting for near-grazing incidence over Neumann boundary conditions, and beam focusing from a permittivity “lens”.

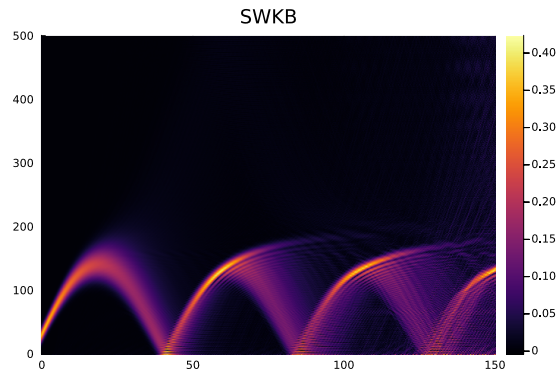


Figure 7: Simplified super-refractive atmospheric conditions

The transport equations, upon replacement of (35) in (17), yields the additional term

$$(x_t, z_t) \cdot \nabla A = -\Delta \Psi A \quad (36)$$

where the left-hand side can be also expressed as a derivative along the rays

$$A_t = -\Delta \Psi A \quad (37)$$

Laplacian on the ray coordinates

In order to solve the first transport equation, we need to obtain an expression for the Laplacian

$$\Delta \Psi(s, t) = \psi_{xx}(x(s, t), z(s, t)) + \psi_{zz}(x(s, t), z(s, t))$$

In the existing literature, this second derivative has been traditionally computed by means of finite differences, which leads to lower orders of accuracy. We introduce an alternative method, based on the system of characteristics (35).

We proceed by taking derivatives with respect to s in (35). Assuming smoothness, we can the interchange the differentiation order to obtain

$$\begin{cases} \partial_t(X_s) = 2P_s \\ \partial_t(Z_s) = 2Q_s \\ \partial_t(\Psi_s) = 2\varepsilon_x X_s + 2\varepsilon_z Z_s \\ \partial_t(P_s) = \varepsilon_{xx} X_s + \varepsilon_{xz} Z_s \\ \partial_t(Q_s) = \varepsilon_{zx} X_s + \varepsilon_{zz} Z_s \end{cases} \quad (38)$$

This ODE system can be integrated if corresponding initial conditions for $(X_s, Z_s, \Psi_s, P_s, Q_s)$ are provided.

To obtain an expression for $\Delta \Psi$, we employ the relations

$$\begin{cases} P_s = \Psi_{xx} X_s + \Psi_{xz} Z_s \\ Q_s = \Psi_{zx} X_s + \Psi_{zz} Z_s \\ P_t = \Psi_{xx} X_t + \Psi_{xz} Z_t \\ Q_t = \Psi_{zx} X_t + \Psi_{zz} Z_t \end{cases} \quad (39)$$

which lead to two independent 2×2 systems needed to solve for $(\Psi_{xx}, \Psi_{xz}, \Psi_{zx}, \Psi_{zz})$:

$$\begin{bmatrix} X_t & Z_t \\ X_s & Z_s \end{bmatrix} \begin{pmatrix} \Psi_{xx} \\ \Psi_{xz} \end{pmatrix} = \begin{pmatrix} P_t \\ P_s \end{pmatrix} \quad (40)$$

$$\begin{bmatrix} X_t & Z_t \\ X_s & Z_s \end{bmatrix} \begin{pmatrix} \Psi_{zx} \\ \Psi_{zz} \end{pmatrix} = \begin{pmatrix} Q_t \\ Q_s \end{pmatrix} \quad (41)$$

These systems have a unique solution under the assumption that the map $(s, t) \rightarrow (X, Z)$ is invertible. Using Cramer's rule, we reach an expression for the Laplacian:

$$\Delta \Psi = \frac{P_t Z_s - Z_t P_s + X_t Q_s - Q_t X_s}{X_t Z_s - Z_t X_s} \quad (42)$$

Denoting the Jacobian of the ray-mapping by

$$J(s, t) = x_t z_s + x_s z_t \quad (43)$$

we note that (42) can also be expressed as

$$\Delta\Psi = \frac{J_t}{J} \quad (44)$$

This implies that an expression for the amplitude can be given in terms of the Jacobian:

$$A(s, t) = \frac{J(s, t)}{J(s, 0)} A(s, 0) \quad (45)$$

can be obtained by adding extra derivatives with respect to s to the ODE system.

References

- [1] Faisal Amlani and Oscar P Bruno. An fc-based spectral solver for elastodynamic problems in general three-dimensional domains. *Journal of Computational Physics*, 307:333–354, 2016.
- [2] Vasilii M Babich and Vladimir Sergeevich Buldyrev. *Short-wavelength diffraction theory: asymptotic methods*. Springer, 1991.
- [3] Max Born and Emil Wolf. *Principles of optics: electromagnetic theory of propagation, interference and diffraction of light*. Elsevier, 2013.
- [4] Oscar P Bruno and Mark Lyon. High-order unconditionally stable fc-ad solvers for general smooth domains i. basic elements. *Journal of Computational Physics*, 229(6):2009–2033, 2010.
- [5] Vlastislav Červený, Mikhail M Popov, and Ivan Pšenčík. Computation of wave fields in inhomogeneous media—gaussian beam approach. *Geophysical Journal International*, 70(1):109–128, 1982.
- [6] Björn Engquist and Olof Runborg. Computational high frequency wave propagation. *Acta numerica*, 12:181–266, 2003.
- [7] RH Hardin. Applications of the split-step fourier method to the numerical solution of nonlinear and variable coefficient wave equations. *SIAM Review (Chronicles)*, 15, 1973.
- [8] Lars Hörmander. *Linear partial differential operators*. Springer, 1963.
- [9] Finn B Jensen, William A Kuperman, Michael B Porter, Henrik Schmidt, and Alexandra Tolstoy. *Computational ocean acoustics*, volume 794. Springer, 2011.
- [10] Joseph B Keller. Geometrical theory of diffraction. *Josa*, 52(2):116–130, 1962.
- [11] Mikhail Aleksandrovich Leontovich and Vladimir Aleksandrovich Fock. Solution of the problem of propagation of electromagnetic waves along the earth’s surface by the method of parabolic equation. *J. Phys. Ussr*, 10(1):13–23, 1946.
- [12] Sheehan Olver and Alex Townsend. A fast and well-conditioned spectral method. *siam REVIEW*, 55(3):462–489, 2013.
- [13] Steven J Ruuth, Barry Merriman, and Stanley Osher. A fixed grid method for capturing the motion of self-intersecting wavefronts and related pdes. *Journal of Computational Physics*, 163(1):1–21, 2000.

- [14] John Steinhoff, Meng Fan, and Lesong Wang. A new eulerian method for the computation of propagating short acoustic and electromagnetic pulses. *Journal of Computational Physics*, 157(2):683–706, 2000.
- [15] Nicolay M Tanushev, Björn Engquist, and Richard Tsai. Gaussian beam decomposition of high frequency wave fields. *Journal of Computational Physics*, 228(23):8856–8871, 2009.
- [16] Ru-Shan Wu. Wide-angle elastic wave one-way propagation in heterogeneous media and an elastic wave complex-screen method. *Journal of Geophysical Research: Solid Earth*, 99(B1):751–766, 1994.